On the relationship between tropospheric CO and CO_2 during KORUS-AQ and its role in constraining anthropogenic CO_2

Tang et al., 2020

Text S1:
Technical details for simulating atmospheric CO_2 explicitly with external CO_2 fluxes in CAM-chem

To add the online CO_2 simulation, we firstly define a new species called "CO2_online" in the model. CAM-chem employs a chemical preprocessor (named chem_mech.in by default) to generate CAM Fortran source code for the chemistry solver, which provides flexibility in defining and changing the chemical mechanism (Lamarque et al., 2012). We define "CO2_online" in the chemical preprocessor to be explicitly solved. The CO_2 fluxes described in Section 2.1 are used as prescribed sources and sinks for the "CO2_online" variable at the surface. We do not explicitly solve the chemical production of CO_2 to total CO_2 in these simulations. Although we added a capability to track the chemical contribution to CO_2 from CH_4 and NMVOCs (including CO) by adding an independent variable called "CO2_chem" in CAM-chem, we will be investigating this variable in the future. For initial conditions, we use the CT2017 mole fraction fields to avoid long spin-up. We also note that the "CO2_online" is a newly added chemical species in CAM-chem with no impact to model physics (such as radiative effect) yet.

Table S1. Summary of all CO_2 fluxes used in this study

CO_2 fluxes	Spatial Res.	Temporal Res.	Period	Transport Model	Fossil Fuel Priors	Biosphere and Fires Priors	Ocean Priors	Main Reference
CAMS (v17r1)	3.75° lon 1.875 ° lat	3-hourly	1979-2017	LMDz[1]	EDGAR scaled to CDIAC	ORCHIDEE (climatology) + GFEDv4	Landschützer et al. (2014)	Chevallier (2018)[2]
CT2017	1° lon 1° lat	3-hourly monthly	2000-2017	TM5	“Miller" (EDGAR scaled to CDIAC) & "ODIAC"	CASA w/ GFED 4.1s GFED_CMS	Jacobson et al. (2007) Takahashi et al (2009)	Peters et al. (2007)[3]
CTE2018	1° lon 1° lat	monthly	2000-2016	TM5	EDGAR+ IER scaled to CDIAC	SiBCASA-GFED4	Jacobson et al. (2007)	van der Laan-Luijkx et al. (2017)[4]

[1]The Laboratoire de Météorologie Dynamique General Circulation Model (LMDz).
[2]Data available at http://apps.ecmwf.int/datasets/data/cams-ghg-inversions.
[3]With updates documented at http://carbontracker.noaa.gov.
[4]Data available at http://www.carbontracker.eu.

Table S2. Global budget of CO_2 (in 10^{15} g C) and CO (in 10^{12} g C) during KORUS-AQ (May 2016).

			CO_2 (PgC)			CO (TgC)
		Region	CT2017	CTE2018	CAMSv17r1	
Sources	fossil fuel or anthropogenic	Korea	0.01	0.01	/	0.11
		Japan	0.02	0.03	/	0.13
		EA-S	0.07	0.07	/	1.68
		EA-M	0.11	0.11	/	2.71
		EA-N	0.05	0.04	/	1.05
		the rest	0.53	0.53	/	18.44
	fire		0.11	0.11	/	9.69
	biosphere		/	/	/	3.25
	ocean		/	/	/	0.61
	chemical production		/	/	/	58.40
	source total		0.90	0.89	/	96.07
Sinks	biosphere		0.63	0.90	/	/
	ocean		0.26	0.18	/	/
	chemical loss*		/	/	/	102.76
	sink total		0.88	1.08	/	102.76
Net (Sources-Sinks)			0.01	-0.19	-0.04	-6.69
Initial Burden			854.83	854.37	853.98	156.82
Final Burden			854.93	854.19	853.93	145.10
Initial-Final			-0.10	0.18	0.05	11.72
Budget delta			-0.08	-0.01	0.01	5.03

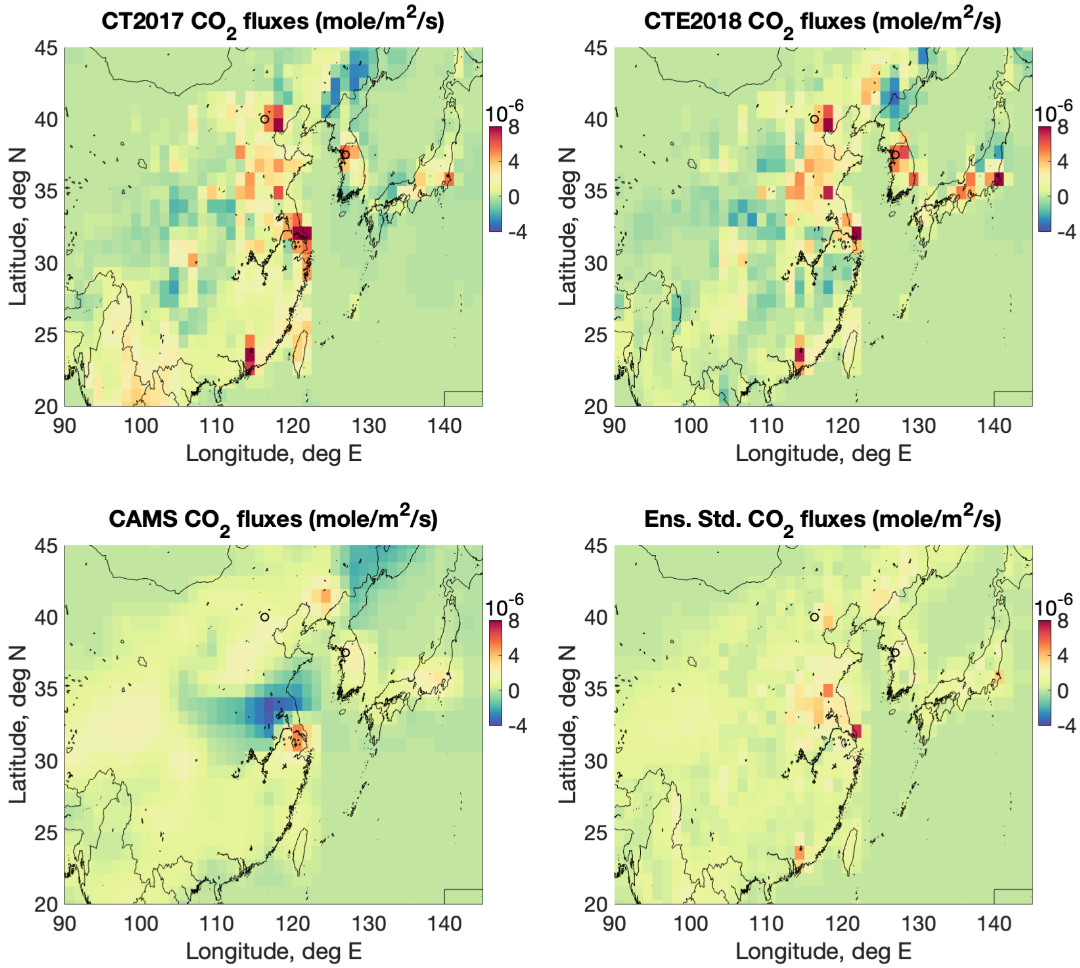

Figure S1. Spatial distribution of monthly-mean (May 2016) *a posteriori* fluxes from CT2017 (top left), CTE2018 (top right), CAMSv17r1 (bottom left), and the corresponding ensemble standard deviation across the three fluxes (bottom right).

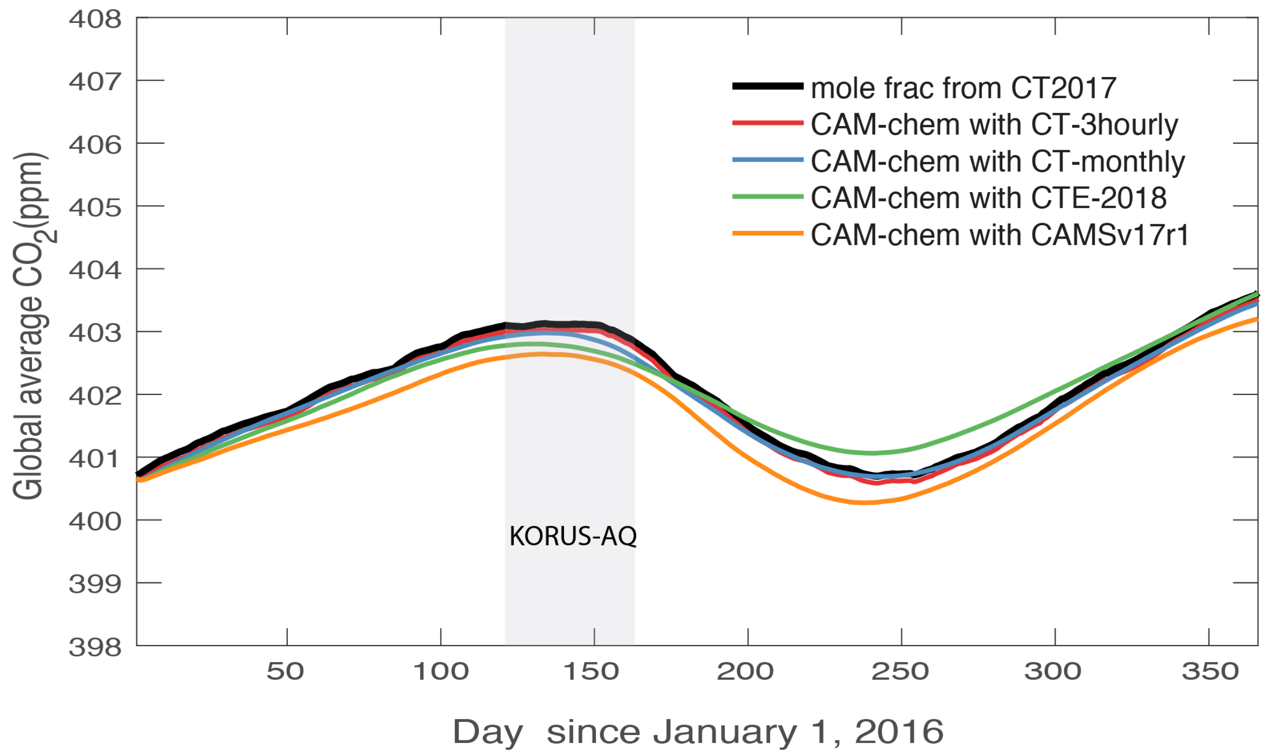

Figure S2. Global average atmospheric CO_2 mixing ratios in 2016 from CT2017 mole fraction fields (black line) and CAM-chem simulations of CO_2 (using fluxes from CT3h, red; CTm, blue, CTE2018, green; and CAMSv17r1, orange). The KORUS-AQ period corresponds to 122-162 days since January 1, 2016.

Other observational datasets used in the study:

Surface flask air sampling. The NOAA ESRL Carbon Cycle Cooperative Global Air Sampling Network is an international effort that includes samples from the NOAA ESRL/GMD baseline observatories, cooperative fixed sites, as well as commercial ships (https://www.esrl.noaa.gov/gmd/ccgg/flask.php). We use the flask measurements of atmospheric CO_2 and CO dry air mole fractions from four ground sites in East Asia that are part of the NOAA ESRL Carbon Cycle Cooperative Global Air Sampling Network (Dlugokencky et al., 2018; Petron et al., 2018), namely Anmyeon-do (AMY), Lulin (LLN), Ulaan Uul (UUM), and Mt. Waliguan (WLG). For comparison, model results are interpolated to the four sites. These datasets serve as the data for baseline comparison and providing seasonal context of the model simulations.

Ground-based remote sensing. The Total Carbon Column Observing Network (TCCON) is a global ground-based network that measure column abundances of CO_2, CO, CH_4, N_2O as well as other species that also absorb in the near-infrared (Wunch et al., 2011; https://tccon-wiki.caltech.edu/). In this study, XCO_2 and XCO measurements from four TCCON sites in East Asia (Release GGG2014) are used (Wunch et al., 2015), including Anmyeon-do (Goo et al., 2017), Saga (Shiomi et al., 2017), Tsukuba (Morino et al., 2017a), and Rikubetsu (Morino et al., 2017b). For comparison, model results are interpolated to TCCON locations and smoothed with TCCON *a priori* profiles and averaging kernels (AKs). These datasets also serve as our data for baseline comparison and consistency check with the corresponding satellite retrievals.

Table S3. Summary of all observations used in this study.

			CO_2	CO
Satellite Retrievals	Orbiting Carbon Observatory-2 (OCO-2)	Date product	Level 2 v8 Lite XCO2	
		Resolution	2.25x1.29 km Global coverage 2x/month	
		Revisit time	1:18 - 1:33 pm	
		Uncertainty	1-2 ppm XCO_2 (Boesch et al., 2011 and references therein)	
	Measurements Of Pollution In The Troposphere (MOPITT)	Date product		TIR/NIR Level 2 v7 XCO
		Resolution		22 x 22 km ~3-4 days
		Revisit time		10:30 AM
		Uncertainty		0.09e18 molec/cm^2 total column retrieval; (Deeter et al., 2014)
NOAA ESRL Carbon Cycle Cooperative Global (CCGG) Air Sampling Network	Anmyeon-do (AMY) 36.54°N, 126.33°E 85.12 masl	Available period Measuring method Data size	2013.12 - now Surface flask air sampling 119 measurements in 2016	
	Lulin (LLN) 23.47°N, 120.87°E 2862.00 masl	Available period Measuring method Data size	2006.08 - now Surface flask air sampling 98 measurements in 2016	
	Ulaan Uul (UUM) 44.45°N, 111.10°E 1007.00 masl	Available period Measuring method Data size	1992.01 - now Surface flask air sampling 104 measurements in 2016	
	Mt. Waliguan (WLG) 36.29°N, 100.90°E 3810.00 masl	Available period Measuring method Data size	1990.08 - now Surface flask air sampling 102 measurements in 2016	
Total Carbon Column Observing Network (TCCON)	Anmyeon-do 36.54°N, 126.33°E 30 masl	Available period Instrument Data size reference	2015.02 - 2016.11 ground-based Fourier Transform Spectrometers 3081 measurements in 2016 Goo et al., 2017	
	Saga 33.24°N, 130.29°E 7 masl	Available period Instrument Data size reference	2011.07 - 2018.08 ground-based Fourier Transform Spectrometers 7177 measurements in 2016 Shiomi et al., 2017	
	Tsukuba 36.05°N, 140.12°E 31 masl	Available period Instrument Data size reference	2011.08 - 2017.12 ground-based Fourier Transform Spectrometers 16499 measurements in 2016 Morino et al., 2017a	
	Rikubetsu 43.46°N, 143.77°E, 380 masl	Available period Instrument Data size reference	2013.11 - 2017.12 ground-based Fourier Transform Spectrometers 6127 measurements in 2016 Morino et al., 2017b	
Measurements during KORUS-AQ	NASA DC-8 aircraft	Team Instrument Time Response Precision Accuracy	AVOCET LI-COR 1 second < 0.1 ppm 0.25 ppm	DACOM/DLH DACOM 1 second < 1% or 0.1 ppb 2%
	Taehwa ground site 37.31°N,127.31°E	Instrument Data intervals	LI-COR LI-7500 1 hour	Thermo 48i 1 hour

Table S4. Summary statistics of CO and CO_2 from surface (in-situ/CCGG, column/TCCON), aircraft (DC-8), and remote sensing (OCO-2, MOPITT) measurements. npair is the number of data pairs of CO and CO_2. Model equivalent and model evaluation against CO and CO_2 data are also shown. Units are ppm for CO_2 and ppb for CO.

		NOAA/ESRL CCGG				TCCON			
		AMY	LLN	UUM	WLG	Amy	Sag	Tsu	Rik
npair		95	64	86	89	3081	7177	6499	6127
Obs Mean	CO_2	415	407	406	405	403	406	403	403
	CO	217	124	142	130	109	108	103	99
Obs Std	CO_2	12	3	6	3	3	2	2	3
	CO	67	55	26	26	8	15	14	15
Obs $R_{CO2,CO}$		0.32	0.31	0.48	0.36	0.59	0.52	0.37	0.28
Obs $\Delta CO/\Delta CO_2$		5.90	18.90	4.53	9.42	2.86	7.40	5.63	4.81
Model Mean	CO_2	414	405	405	406	403	405	404	403
	CO	239	142	129	187	105	111	102	93
Model Std	CO_2	6-8	2	6-8	5-7	2-3	~2	~2	3-4
	CO	124	103	52	173	12	19	17	20
Model $R_{CO2,CO}$ (min/max)		-0.12	0.46	0.16	0.40	-0.2	0.51	0.33	0.05
		0.18	0.70	0.27	0.71	-0.1	0.54	0.44	0.29
Model $\Delta CO/\Delta CO_2$ (min/max)		21.01	48.85	6.64	33.88	/	9.53	7.43	5.57
		26.17	59.80	8.68	44.47		11.24	8.67	7.53
Bias Model minus Obs	CT3h	-0.2	-1.4	-0.6	-0.1	-0.6	-1.0	0.9	-0.1
	CTm	-0.2	-1.4	-0.7	0.3	-0.2	-1.0	1.1	0.2
	CTE2018	1.4	-1.2	-0.3	1.5	0.5	-0.6	1.6	0.6
	CAMS	-3.4	-1.6	-1.0	0.1	-0.9	-1.5	0.3	-0.5
	CT2017 CO	22.0	18.1	-13.7	57.1	-4.3	2.3	-0.9	-6.1
R Model versus Obs	CT3h	0.74	0.46	0.84	0.83	0.92	0.85	0.87	0.94
	CTm	0.70	0.71	0.86	0.81	0.92	0.87	0.86	0.94
	CTE2018	0.81	0.62	0.88	0.69	0.91	0.86	0.84	0.91
	CAMS	0.67	0.67	0.92	0.82	0.92	0.86	0.89	0.95
	CT2017 CO	0.68	0.92	0.21	0.22	0.40	0.63	0.61	0.66
RMSE	CT3h	8.1	3.0	4.5	4.4	1.3	1.5	1.5	1.2
	CTm	8.6	2.5	3.3	2.8	1.2	1.4	1.6	1.1
	CTE2018	7.4	2.6	3.0	4.0	1.4	1.2	2.1	1.4
	CAMS	9.7	2.7	2.7	2.6	1.5	1.8	1.2	1.1
	CT2017 CO	94.6	59.0	54.7	177.9	12.1	15.5	14.1	16.2
errorR	CT3h	0.43	0.17	0.43	0.49	0.10	0.31	0.15	0.01
	CTm	0.41	0.32	0.46	0.62	0.07	0.30	0.19	0.40
	CTE2018	0.47	0.36	0.50	0.84	0.34	0.30	0.34	0.56
	CAMS	0.54	0.13	0.48	0.79	0.13	0.31	0.22	0.43

Observed and modeled CO_2 and CO at NOAA CCGG sites in the region

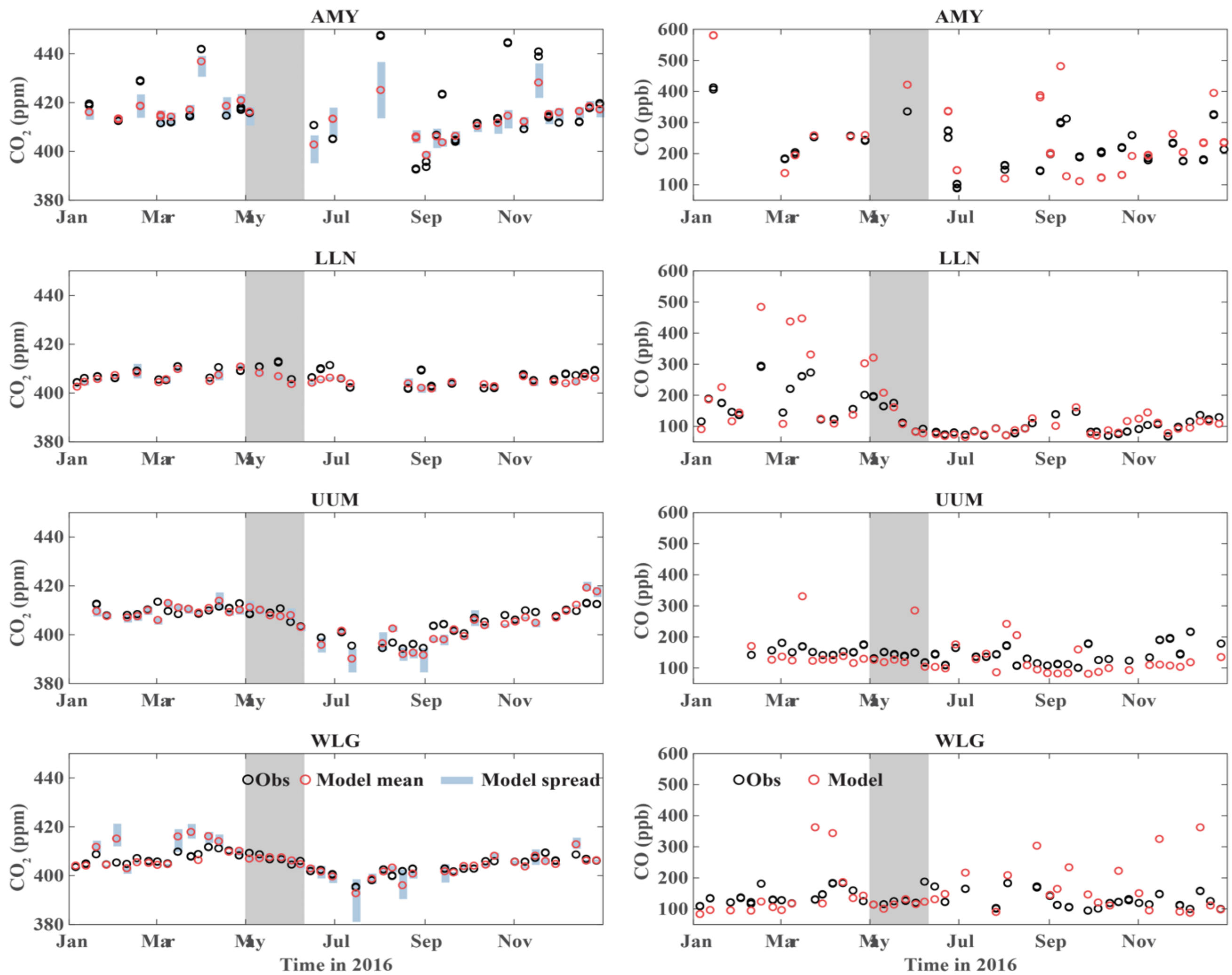

Figure S3. Time series of CO_2 data (left panel) and CO data (right panel) in black dots superimposed with the corresponding model results (red dots) at four East Asia sites from the NOAA ESRL Carbon Cycle Cooperative Global (CCGG) Air Sampling Network in 2016. The equivalent modeled CO_2 is represented as the mean of four model simulations with the blue bars representing the spread (min/max) of the four model simulations) The KORUS-AQ period (May 1 – June 10) is indicated in gray shade.

Observed and modeled CO_2 and CO at TCCON sites in the region

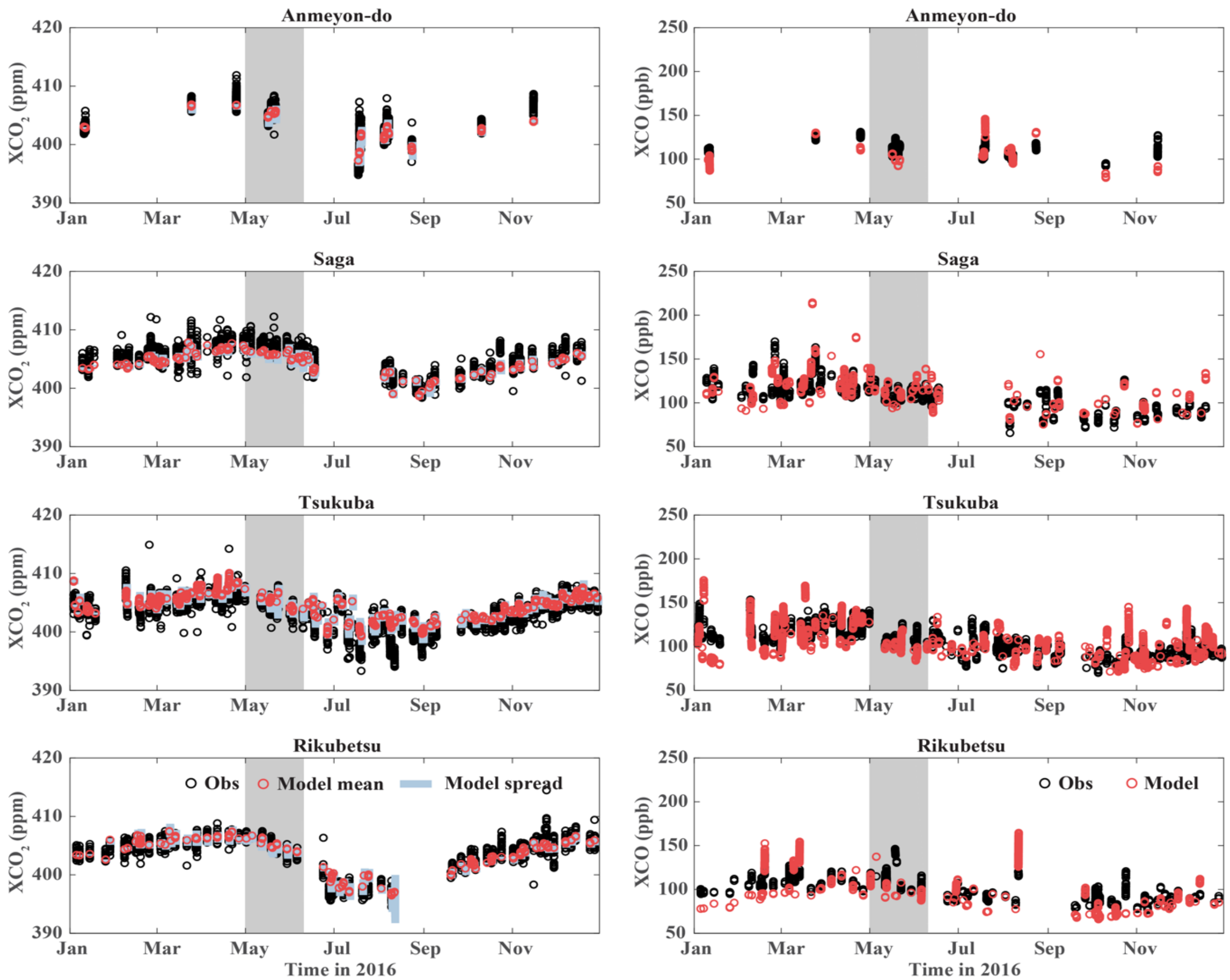

Figure S4. Time series of observations (black dots) and corresponding model results (red dots) The equivalent modeled CO_2 is represented as the ensemble mean of four model simulations with the blue bars representing the spread (min/max) of the four model simulations at four TCCON sites in 2016. KORUS-AQ period (May 1 – June 10) is indicated in gray shade.

Observed and modeled XCO_2 and XCO in the region

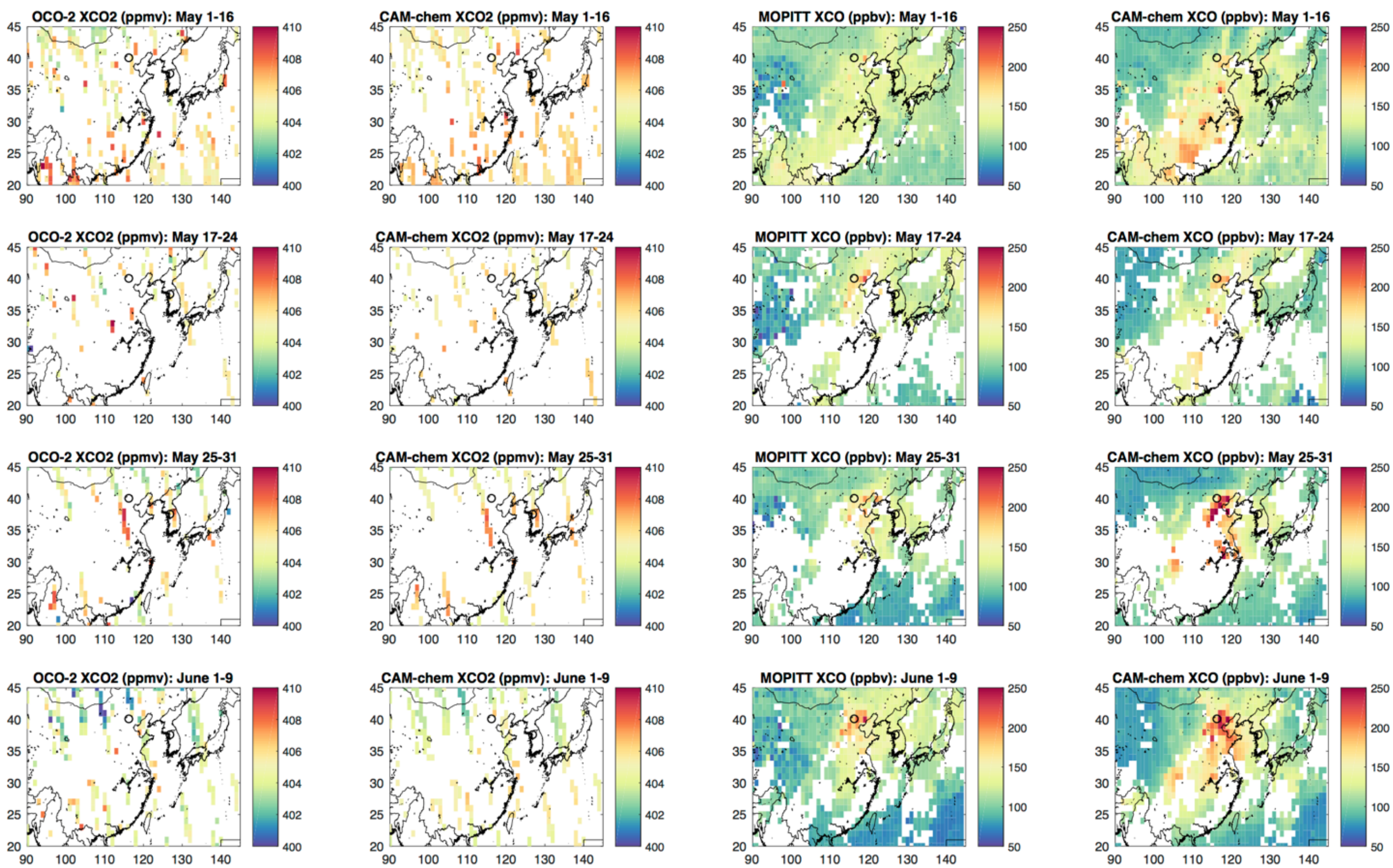

Figure S5. Comparison CAM-Chem results with CO_2 and CO satellite data (similar to Figure 2 of main text but for specific periods during the campaign). Panels in the first column correspond to the mean OCO-2 XCO_2 column density across KORUS-AQ period (ppm) and equivalent XCO_2 averaged across four model simulations in the second column). Panels in the third column correspond to MOPITT XCO column density averaged across KORUS-AQ period (ppb) and equivalent XCO (fourth column).

Tagging $ffCO_2$ and CO

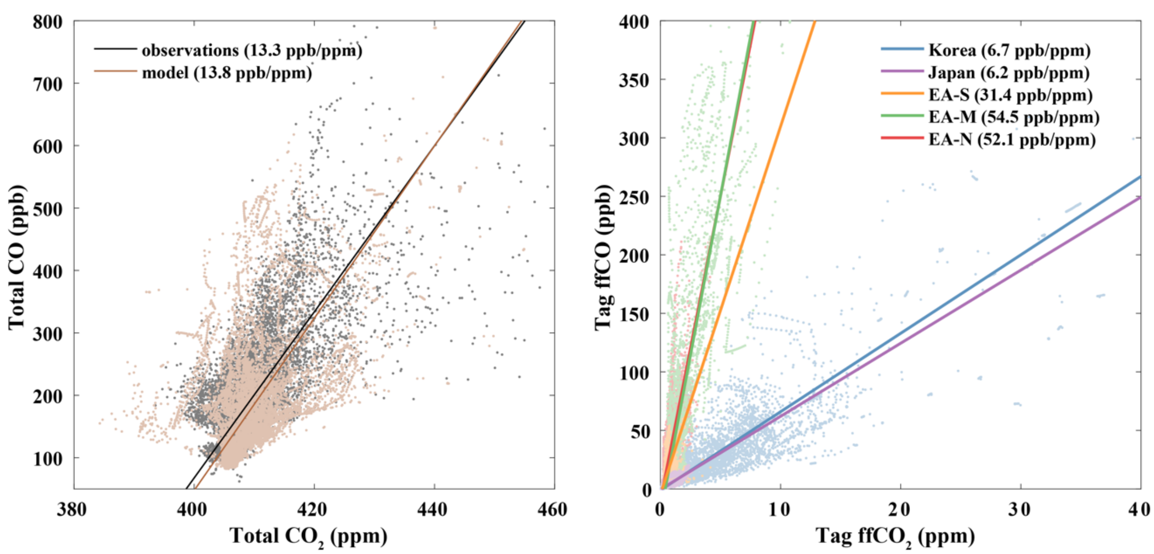

Figure S6. Comparison between observed (black) and modeled (brown) total CO_2 and CO mixing ratios (left panel) and corresponding association of modeled ffCO and $ffCO_2$ tags in CAM-Chem.

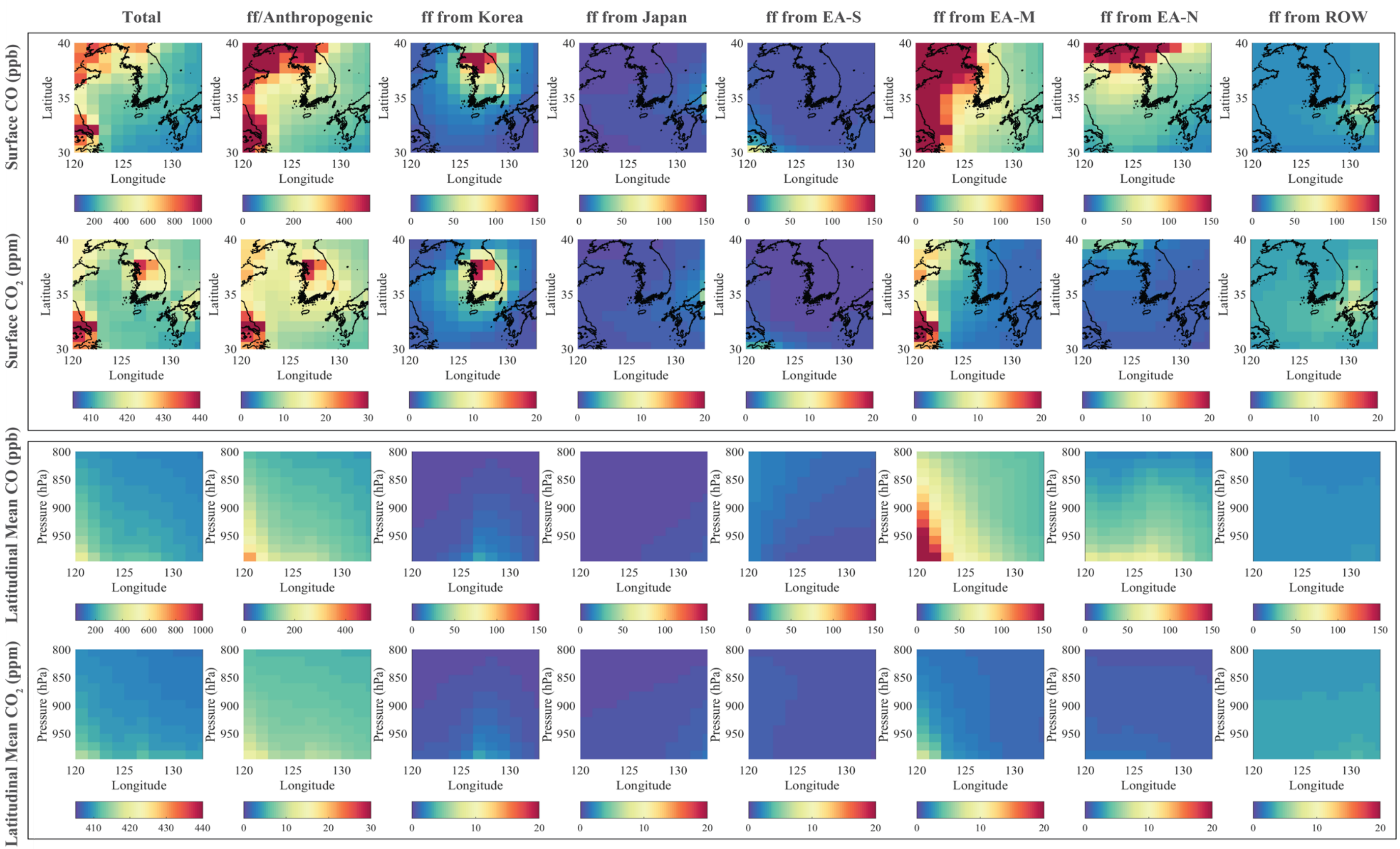

Figure S7. Spatial distribution of CO_2 and CO over Seoul and nearby regions. This is shown in the different columns for total CO_2 (or CO), its associated $ffCO_2$ (or ffCO) and regional contributions at the surface (top), along with corresponding mean zonal distributions averaged across KORUS-AQ domain (bottom).

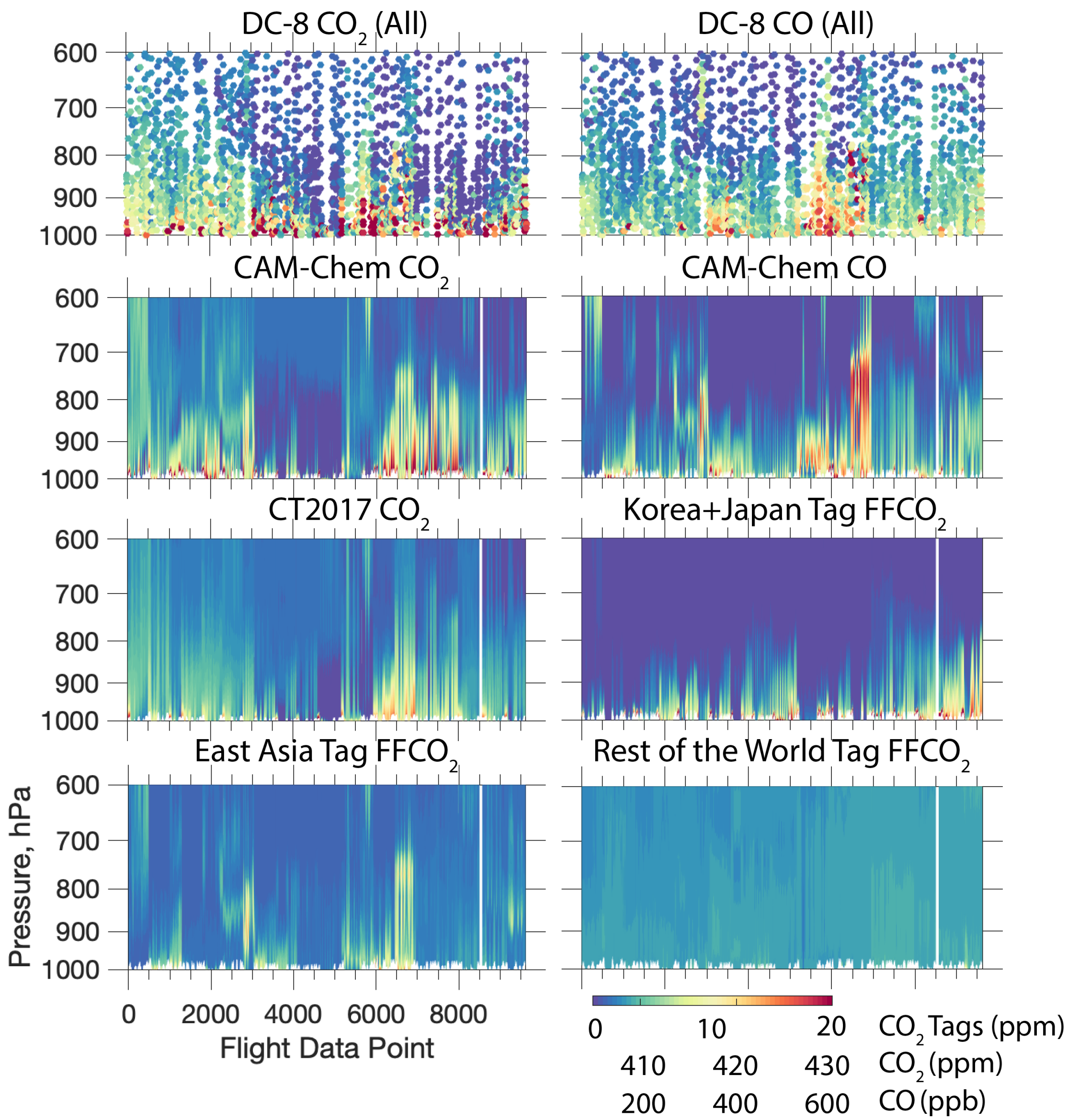

Figure S8. KORUS-AQ flight curtains for DC-8 CO_2 and CO (top row) and for CAM-Chem model equivalent (second row) and for Carbon Tracker CO_2 files (CT3h, third row, left panel). These curtains correspond to all flight data points of the campaign (flight group:All). Also shown are corresponding contributions of a priori $ffCO_2$ response functions from Korea+Japan (third row, right panel), East Asia (fourth row, left) and Rest of the World (fourth row, right).

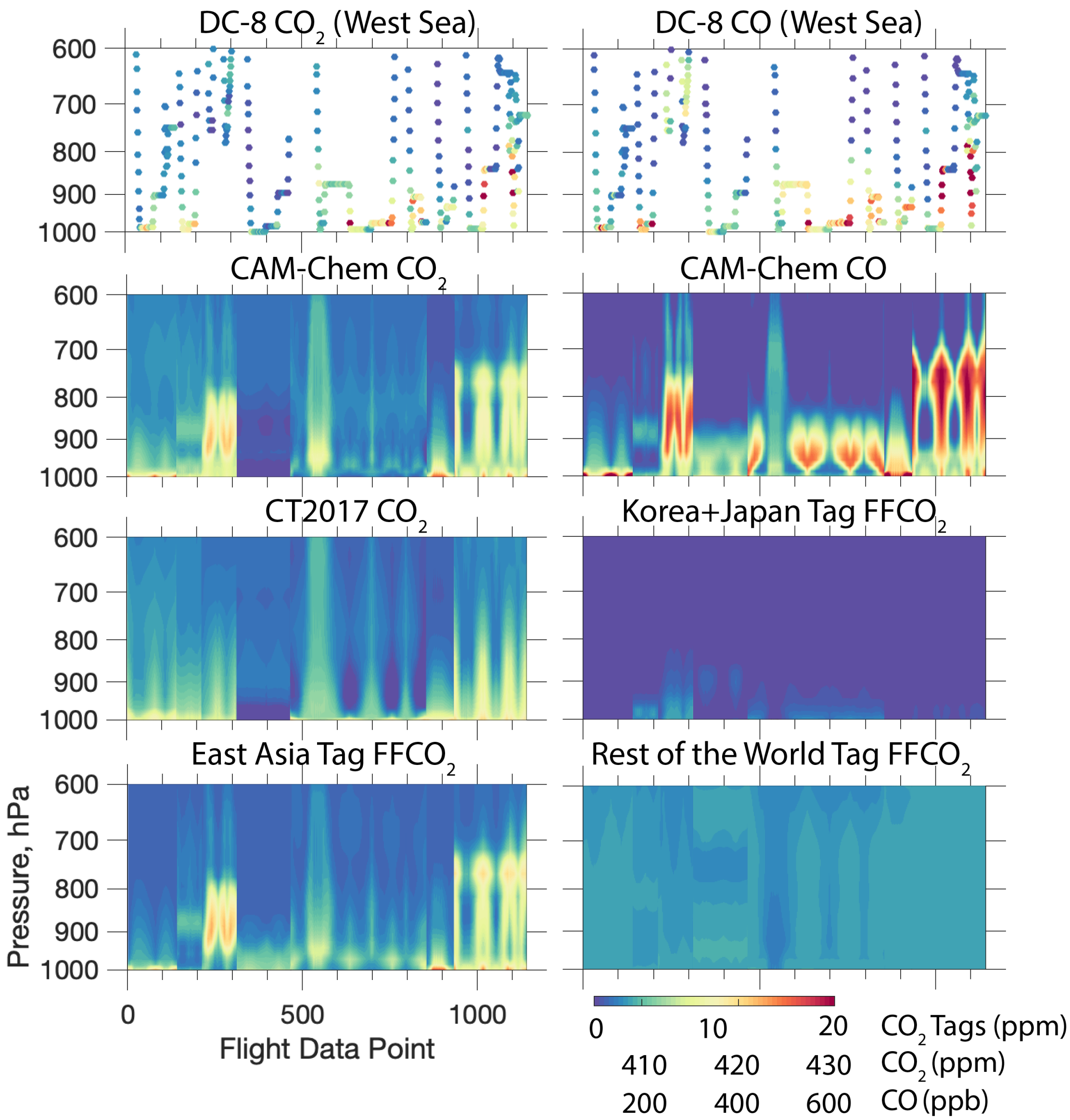

Figure S9. Same as Figure S7 but for West Sea flight group.

Other References (not cited in main text)

Morino, I., T. Matsuzaki, A. Shishime.: TCCON data from Tsukuba, Ibaraki, Japan, 125HR, Release GGG2014R2. TCCON data archive, hosted by CaltechDATA, California Institute of Technology, Pasadena, CA, U.S.A. http://doi.org/10.14291/tccon.ggg2014.tsukuba02.R2, 2017a.

Morino, I., N. Yokozeki, T. Matzuzaki, A. Shishime.: TCCON data from Rikubetsu, Hokkaido, Japan, Release GGG2014R2. TCCON data archive, hosted by CaltechDATA, California Institute of Technology, Pasadena, CA, U.S.A. https://doi.org/10.14291/tccon.ggg2014.rikubetsu01.R2, 2017b.

Oh, Y.S., Kenea, S.T., Goo, T.Y., Chung, K.S., Rhee, J.S., Ou, M.L., Byun, Y.H., Wennberg, P.O., Kiel, M., DiGangi, J.P. and Diskin, G.S.: Characteristics of greenhouse gas concentrations derived from ground-based FTS spectra at Anmyeondo, South Korea, *Atmospheric Measurement Techniques*, *11*, 2361-2374, 2018.

Landschützer, P., Gruber, N., Bakker, D.C. and Schuster, U.: Recent variability of the global ocean carbon sink. *Global Biogeochemical Cycles*, *28*(9), 927-949, 2014.

Petron, G., Crotwell, A.M., Lang, P.M., Dlugokencky, E.: Atmospheric Carbon Monoxide Dry Air Mole Fractions from the NOAA ESRL Carbon Cycle Cooperative Global Air Sampling Network, 1988-2017, Version: 2018-10-17, Path: ftp://aftp.cmdl.noaa.gov/data/trace_gases/co/flask/surface/, 2018.

Wunch, D., Toon, G. C., Blavier, J. F. L., Washenfelder, R. A., Notholt, J., Connor, B. J., Griffith, D. W., Sherlock, V., and Wennberg, P. O.: The total carbon column observing network, *Philosophical Transactions of the Royal Society A*, 369, 2087–2112, 2011.